Comparison of Slab Thermal Stresses in Methane- vs. Hydrogen-Fired Reheating Furnace Operations With Computational Fluid Dynamics

While the effectiveness of hydrogen fuel usage for carbon emission reductions is well-known, the potential secondary effects of hydrogen usage in steel production are still a large focus of research. This article presents a computational fluid dynamics study comparing the thermal stresses in slabs reheated in methane-fired, hydrogen-fired and blended-fuel reheating furnaces. The simulations investigate the effects of different fuel types on the thermal behavior of the slabs and the resulting thermal stresses. The results provide insights on temperature distributions and thermal gradients in the slabs, as well as the associated stresses, for both methane- and hydrogen-fired operations.

Authors

Muhammad Basil Lutfi, Center for Innovation Through Visualization and Simulation, Purdue University Northwest, Hammond, Ind., USA

Nicholas J. Walla (top left), Senior Research Engineer, Center for Innovation Through Visualization and Simulation, Purdue University Northwest, Hammond, Ind., USA

Abhishek Kolakotla, Center for Innovation Through Visualization and Simulation, Purdue University Northwest, Hammond, Ind., USA

Armin K. Silaen (top right), Associate Research Professor, Center for Innovation Through Visualization and Simulation, Purdue University Northwest, Hammond, Ind., USA

Kurt Johnson, Research Engineer, Cleveland-Cliffs Burns Harbor, Burns Harbor, Ind., USA

Chenn Q. Zhou (bottom), NIPSCO Distinguished Professor of Engineering Simulation; Founding Director, Center for Innovation Through Visualization and Simulation; and Founding Director, Steel Manufacturing Simulation and Visualization Consortium, Purdue University Northwest, Hammond, Ind., USA
czhou@pnw.edu

Introduction

Reheat furnaces are integral to industrial processes, particularly in heating steel slabs to requisite temperatures for subsequent deformation in rolling mills. Traditionally, these furnaces operate using fossil fuels like natural gas, which are significant contributors to greenhouse gas (GHG) emissions and how hydrogen is a promising alternative.[1] The pressing global mandate to mitigate carbon footprints has propelled industries to explore alternative fuels, with hydrogen emerging as a promising candidate. Hydrogen combustion yields only water vapor, positioning it as a potential solution for reducing GHG emissions in industrial heating applications. However, integrating hydrogen into reheat furnace operations necessitates a thorough examination of its impact on thermal performance and the resultant thermal stresses on steel slabs to ensure both operational efficiency and material integrity.

The combustion characteristics of hydrogen differ markedly from those of natural gas, influencing flame temperature, heat distribution and energy density within the furnace. These variations can lead to altered temperature gradients across the slabs, potentially inducing localized thermal stresses that may cause cracks, distortions or other mechanical failures. Maintaining an optimal equivalence ratio and determining appropriate blending proportions of hydrogen with natural gas are crucial to achieving a balance between emission reductions and effective heat transfer. Recent research has delved into the feasibility of hydrogen as an industrial fuel, focusing on its combustion properties and energy efficiency. For instance, studies have investigated the combustion dynamics of hydrogen-natural gas blends in reheat furnaces, highlighting the potential for significant CO_2 emission reductions.[2]

Additionally, the use of regenerative burners in conjunction with hydrogen fuel has been evaluated for enhancing thermal efficiency in reheat furnaces.[3] However, there remains a lack of research specifically addressing the thermal and stress responses of steel slabs subjected to varying hydrogen blends in reheat furnaces. Understanding these responses is vital for ensuring that the transition to hydrogen-enriched combustion does not compromise slab quality or furnace performance. Computational fluid dynamics (CFD) modeling, coupled with structural simulations, offers a robust framework for assessing the effects of different combustion conditions on heat transfer and thermal stresses experienced by slabs. Such methodologies have been employed to simulate the combustion of hydrogen in reheat furnaces, providing insights into temperature distributions and potential stress concentrations.[4] Numerical modeling has been utilized to evaluate the thermal performance of regenerative slab reheat furnaces operating with hydrogen fuel, underscoring the importance of precise control over combustion parameters to mitigate adverse thermal stresses.[5]

The reheat furnace is the most energy-intensive process during the entire hot rolling.[6] This study aims to conduct a comprehensive thermal and stress analysis of steel slabs within a reheat furnace operating with various hydrogen-natural gas blends. By employing CFD and structural simulations, the research will identify the impact of hydrogen fuel usage on slab temperature profiles and the associated thermal stresses. The investigation will encompass hydrogen blends ranging from 0% to 100% by burner power, with 25% increments, while maintaining consistent equivalence ratios and operating conditions to isolate the effects of fuel composition. The outcomes are expected to inform optimized furnace designs and operational strategies that facilitate the adoption of hydrogen as a sustainable fuel alternative without compromising material integrity or process efficiency.

Figure 1

Indiana Harbor reheat furnace.

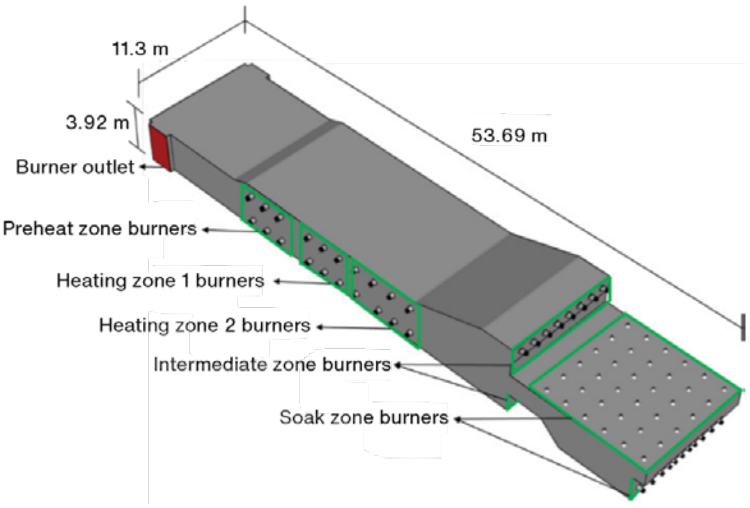

Figure 2

Indiana Harbor reheat furnace.

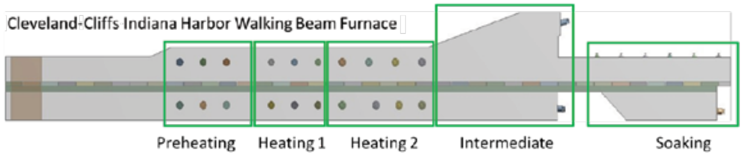

Figure 3

Thermocouple locations.

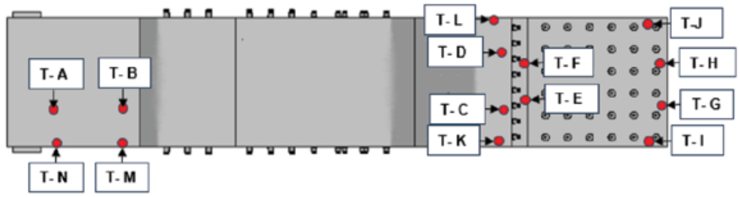

Theory and Methodology

Geometry and Boundary Conditions

The reheating furnace analyzed in this study is located at Cleveland-Cliffs Indiana Harbor. It is a walking beam furnace with overall dimensions of 53.69 m × 11.96 m × 7.6 m, as illustrated in Fig. 1. The furnace operates with a total power input of approximately 125 MW, fueled by natural gas. It is divided into five zones equipped with burners: the preheat zone, the heating zone 1, the heating zone 2, the intermediate zone and the soak zone. A side-view schematic (Fig. 2) provides a detailed depiction of these zones. The furnace employs swirl burners, each featuring one fuel port, four primary inlet ports and eight secondary inlet ports. The preheat zone and heating zone 1 are equipped with 12 burners each, heating zone 2 has 16 burners, and the soak zone contains 36 burners.

The slabs modeled within the furnace have dimensions of 1.27 m × 7.79 m × 0.24 m and are evenly spaced. Arranged in a staggered format, the slabs are transported along the x-axis within the furnace using walking beams. The slabs are loaded from the left side (as shown in Fig. 2) and discharged from the right. Thermocouples are strategically placed throughout the furnace to measure and monitor temperature conditions, with Fig. 3 highlighting their specific locations for validating the CFD model.

For the steady-state simulation, a total of 40 slabs were included in the furnace. The geometry was meshed using tetrahedral elements, which were later converted to polyhedral elements using FLUENT, resulting in a total cell count of approximately 8.3 million. The baseline scenario replicates the operational conditions of the actual furnace, utilizing natural gas as the fuel source. The study also explores hydrogen blends at incremental levels of 25%. The blending methodology involves fuel blending by power, meaning a 25% hydrogen blend implies that 25% of the burner power is supplied by hydrogen. The equivalence ratio remains consistent across the baseline and all hydrogen blends.

The boundary conditions applied to the furnace are designed to closely replicate real-world operating conditions. The furnace walls are constructed from refractory material and are modeled with a convection boundary condition on their external surfaces. The skids inside the furnace are water cooled, and this is simulated by applying a volumetric energy source term to the bottom cell layer of the skids. The boundary conditions for each burner zone are summarized in Table 1. The mass flowrates are taken from a time-averaged of data which was provided by Cliff's and represents normal operating conditions with 80% load in the furnace. The inlet temperatures for natural gas and air are set at 300 K and 640 K, respectively. Table 2 details the mass flow rates of hydrogen for the different blend cases. For each case, the total power input was kept identical.

Fluid and Combustion Modeling: To simulate the flow characteristics and combustion in the reheat furnace, the following equations for continuity, mass, momentum, turbulence and species transport equations are solved using Fluent, a commercial CFD solver. The description of equations used and their implementation can be found in the ANSYS Fluent Theory Guide.[7] Flow turbulence was modeled using the k-ω SST turbulence model, with species transport and the Finite-Rate/Eddy Dissipation reaction model. Radiation is calculated using the Discrete Ordinates (DO) method.

Thermal Stress Modeling: ANSYS Workbench Mechanical, the software used to conduct thermal stress analysis, solves the governing equations for slab stress simulation in order to describe the mechanical behavior of a slab subjected to thermal and structural loads. These equations incorporate the distribution of stress, strain and displacement within the slab, which are influenced by temperature gradients and material properties. The solution for thermal stress modeling requires valid slab temperature distributions, which cannot be obtained directly from the steady-state CFD solution. As such, a steady-transient iterative process is performed to cycle between steady-state solutions that resolves combustion behavior and fluid temperature fields and transient solutions that resolve the solid temperature fields.

In the transient simulation, the flow field and furnace temperatures were kept fixed but allowed the slab temperatures to change dynamically. The simulation was run in 30-second intervals for a total of 300 timesteps, which represented the full run time of the furnace. After 420 seconds of simulated time, the slab temperatures were interpolated for the next two billets

Table 1

Air and Fuel Flowrates for Baseline Natural Gas Case

Zone	Natural gas mass flowrate (kg/sec.)	Air mass flowrate (kg/sec.)
Preheat zone top	0	0.76
Preheat zone bottom	0	1.00
Heat zone 1 top	0.34	7.33
Heat zone 1 bottom	0.37	7.86
Heat zone 2 top	0.51	11.32
Heat zone 2 bottom	0.56	11.34
Intermediate zone top	0.21	4.47
Intermediate zone bottom	0.29	5.88
North soak zone top	0.09	1.97
North soak zone bottom	0.1	2.29
South soak zone top	0.14	2.67
South soak zone bottom	0.14	3.00

Table 2

Fuel Flowrates for Hydrogen Blend Case

Blend case by power %	Fuel H_2 mass %	Total fuel (kg/sec.)
100% CH_4	0%	2.75
25% H_2	11%	2.32
50% H_2	28%	1.89
75% H_2	53%	1.47
100% H_2	100%	1.05

to mimic how slabs progress through the furnace, known as the "marching phenomenon." Once the transient simulation was complete, its results were used to run another steady-state simulation. This cycle of transient and steady-state simulations was repeated until the results converged. Convergence was defined as slab temperature differences being less than 3.5% compared to the previous transient cycle. Once this point was achieved, the results were exported to ANSYS Workbench for further analysis.

In Workbench, the first 10 odd-numbered slabs were analyzed. Previous studies had shown that slab stresses tend to be highest in the first half of the furnace. Data such as the average equivalent stresses across these slabs were collected and the cross-sectional stresses caused by thermal expansion and contraction were studied. This approach allowed for a clear picture to emerge of how slabs behave thermally and mechanically as they move through the furnace.

A rudimentary three-step combustion mechanism was used for the CH_4 and H_2 blends, effectively one step for H_2. Although a more detailed mechanism would be ideal, the three-step mechanism was validated against industry data inside the furnace. The boundary conditions and contacts applied during the simulation included fixed supports, the influence of gravity, and a frictional contact between the slab and skid with a coefficient of friction (μ=0.74). Fig. 4 shows the workflow to simulate the slab temperature and thermal stress. The loads were applied through the slab temperature profiles, which were defined for each slab position in sequential steps. These temperature profiles were interpolated from the CFD mesh to the finite element analysis (FEA) mesh to ensure consistency and accuracy in the thermal and structural analysis.

Figure 4

Thermal analysis workflow.

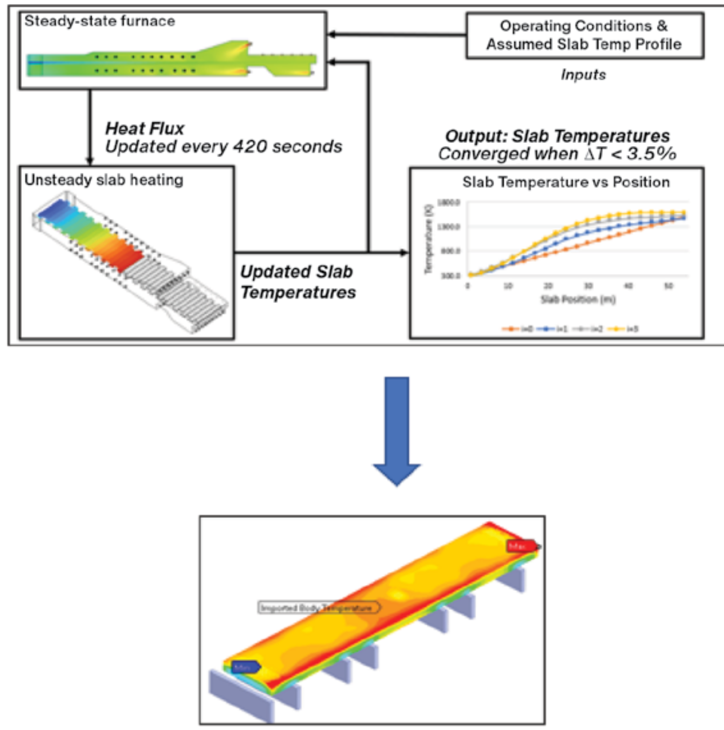

observed is near the floor region at outlet of flue gases. This error could be attributed to a modification to the furnace interior not included in the CFD and which may have altered the flow and heat near the thermocouple.

Full Furnace TC Comparison of All Five Blends

The five different fuel blends were analyzed using the steady-transient iteration cycle until convergence was achieved. The results showed that temperatures increased as the hydrogen percentage in the fuel blend rose. For the 100% hydrogen case, peak temperatures were observed to be approximately 14% higher than those

Results and Discussion

Validation

The CFD model of the Indiana Harbor reheat furnace was validated with the thermocouple (TC) measurements for the thermocouple location, as shown in Fig. 3. The thermocouples in computational domain showed an average error of less than 6% for the given measurement data. This successfully validates the model with the actual furnace. The Fig. 5 shows the actual thermocouple reading vs. the CFD thermocouple value. The highest error

Table 3

Reaction Mechanism for Fuels

Reactions	Pre-exponential factor A (1/sec.)	Activation energy E (J/mol)
$CH_4 + 3/2\ O_2 \rightarrow CO + 2H_2O$	5.012×10^{11}	2.0×10^{8}
$CO + 1/2\ O_2 \rightarrow CO_2$	2.239×10^{12}	1.7×10^{8}
$H_2 + 1/2\ O_2 \rightarrow H_2O$	9.87×10^{8}	3.1×10^{7}

Figure 5

Thermocouple temperature comparison computational fluid dynamics (CFD) vs. industry data.

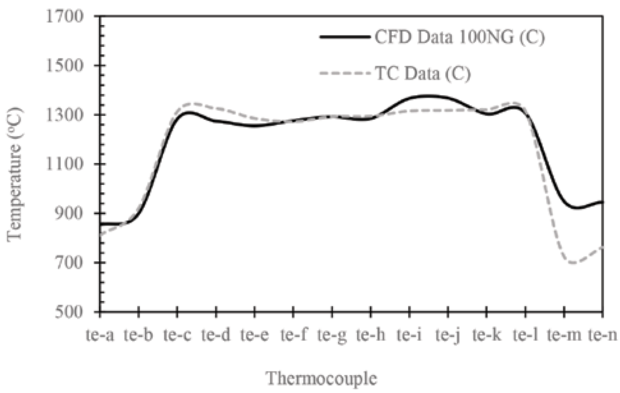

Figure 6

Full furnace thermocouple data for all five blends.

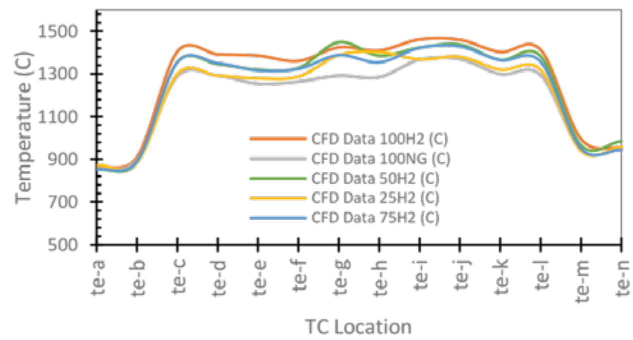

achieved with the base methane (CH_4) case. Interestingly, flue gas temperatures showed minimal variation across the blends, with a maximum difference of only about 1%. The most significant temperature differences were identified in the heating zone of the furnace, where the impact of higher hydrogen content was more pronounced. These elevated temperatures suggest that products within the furnace are likely to experience overheating when higher hydrogen percentages are used, particularly in zones where heating is already intensive.

An energy balance study was then conducted, which revealed out of the total energy going in which was uniform across all five blends, Hydrogen having more radiative heat transfer, was causing a higher percentage of energy going to the slabs. For the 100% natural gas (NG) case, only 48% energy went to the slabs vs. 56% for the 100 H_2 case.

Slab Heat Flux Comparison

As the hydrogen percentage in the fuel blend increases, the heat flux to the slab also rises, indicating a direct correlation between hydrogen content and thermal transfer efficiency. Specifically, the average heat flux at the top of the slab shows a 12% increase when transitioning from 100% NG to 100% hydrogen (H_2). This increase in heat flux is particularly evident along the length of the slab as the hydrogen percentage grows, primarily due to the longer flames produced by hydrogen combustion in this scenario, which also contributed to higher heat flux on the slab surfaces. These combined effects highlight the impact of hydrogen on heat transfer characteristics, making it a key factor in furnace design and operation.

Slab Temperature Comparison

The analysis of temperature probe plots revealed key differences in slab and gas temperatures across different fuel compositions. A centerline temperature profile was

Figure 7

Slab top surface average heat flux comparison.

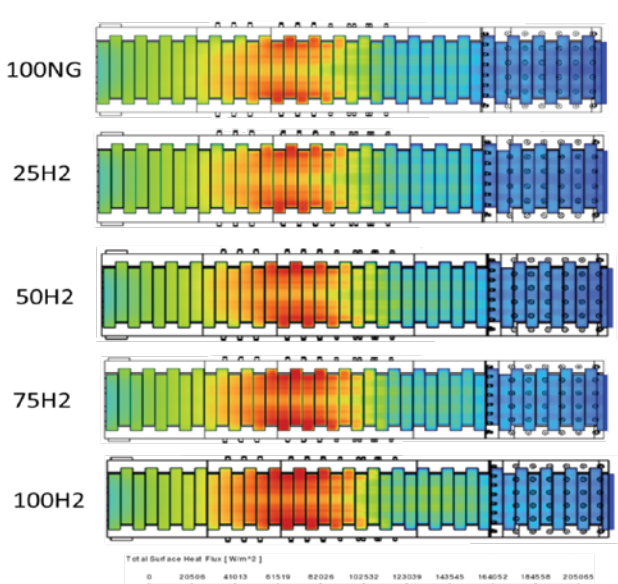

Figure 8

Slab top surface average heat flux comparison.

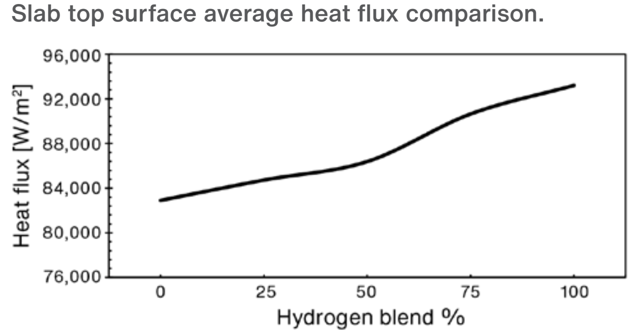

plotted through slabs 1 to 41 to examine the thermal behavior under varying fuel blends. The results showed that when 100% hydrogen (H_2) was used as the fuel, the volume-averaged slab temperatures at the outlet were 96 K higher compared to those obtained using 100% NG. Similarly, the core probe temperatures at the outlet demonstrated an increase of 89 K for 100% hydrogen compared to natural gas, further confirming the significant impact of hydrogen on slab heating.

To identify thermal gradients and pinpoint areas with the largest differences between core and surface temperatures, an analysis was conducted comparing the slab's top surface temperatures to its core temperatures. The temperature differences between these two regions were calculated and plotted to provide a clear visualization of how the thermal gradient evolved throughout the slabs' journey in the furnace. This analysis revealed that the highest core-to-surface temperature difference occurred around slab 12 for all five blends, ranging from 350 to 386 K, highlighting a significant thermal gradient at this stage. As the slabs progressed further through the furnace and approached the exit, the temperatures began to equalize, resulting in a much more uniform thermal distribution. By the time the slabs exited the furnace, the temperature difference between the core and surface had decreased dramatically, dropping to a minimal 14 K.

Slab Equivalent Stresses

To simplify the calculation, the stress data for only the first 10 odd-numbered slabs in the furnace were modeled. In all cases, the highest stresses were found in the preheat zone (PHZ), located about 3.4 m from the charge. This area experiences a combination of thermal and mechanical loads that make it a critical point for stress development in the slabs. Among the various fuel blends analyzed, the 25% hydrogen (25 H_2) case showed the highest stress, reaching 268 MPa, indicating that even partial replacement of natural gas with hydrogen can significantly impact stress levels. When looking at average stress values, they were nearly identical across all cases until the slabs entered heating zone 1 (HZ1). However, as the slabs moved through HZ1, differences in stress values began to emerge and continued to grow. This suggests that the transition from the PHZ to the heating zone plays a key role in how stresses develop, likely influenced by changing heat flux and thermal gradients. These results highlight the need to carefully monitor stress behavior in different zones of the furnace, especially when introducing hydrogen into the fuel mix. As the slabs progress through the HZ1 into HZ2, the max and average stresses reduce to minimal values, hence cut off from the plot. As the yield strength was 290 MPa, all five blends were withing elastic deformation ranges.

Despite the earlier observation in Fig. 10, where the maximum thermal gradient was found around slab 12, the highest stress peak was observed around slab 3. This discrepancy prompted an investigation into the magnitude of the thermal heating at this location. To better understand the relationship, a rationalized temperature difference was calculated between the top surface and the core of the slab, normalizing it to the slab core temperature. This allowed for the thermal difference to be determined as a percentage, which revealed that slab 3 experienced the highest thermal differential in the furnace. Interestingly, this thermal trend aligns perfectly with the observed trends in both the maximum and average stress values. Slab 3 not only showed the largest temperature differential but also corresponded to the highest stress levels.

As the slabs progressed further through the furnace, the stresses gradually decreased as the temperature distribution became more uniform. This homogenization of temperatures significantly reduced the thermal gradients and, consequently, the stresses experienced by the slabs.

Figure 9

Volume average temperatures for slabs.

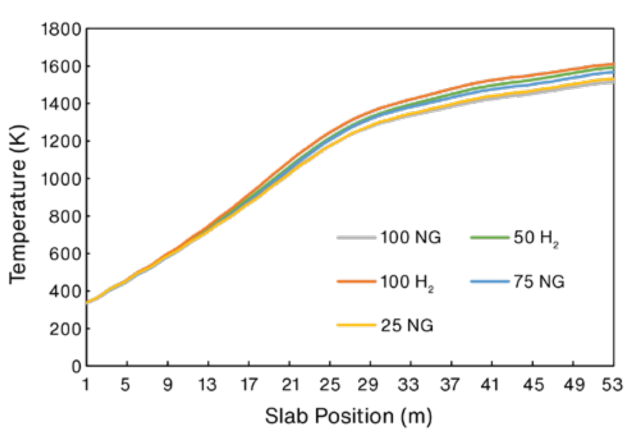

Figure 10

TOP-core temperature plot.

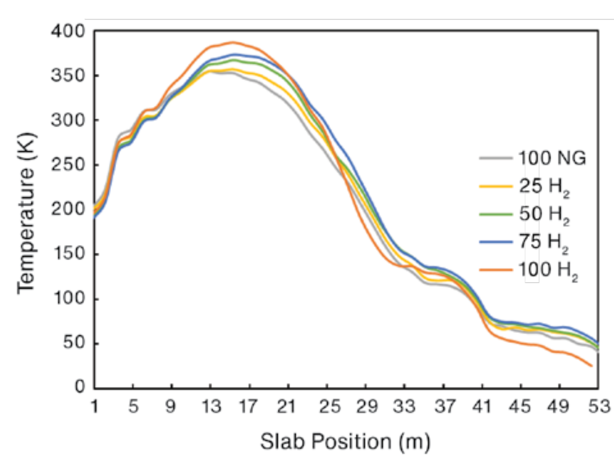

Figure 11

Max. stress and avg. stress at each slab position.

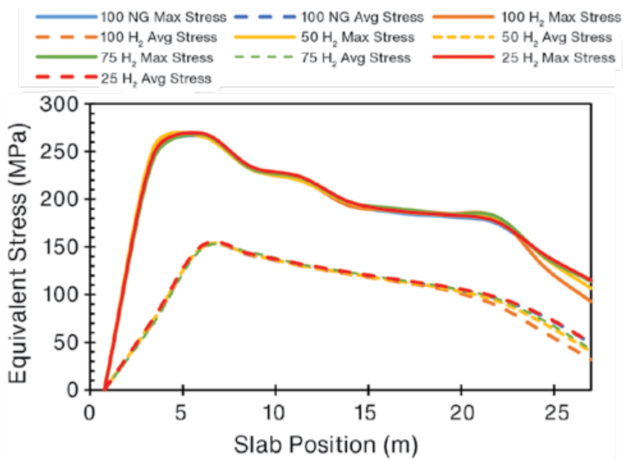

Figure 12

Normalized TOP-core temperature plot.

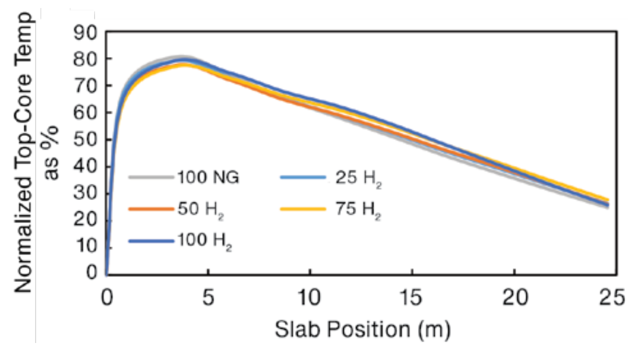

These findings emphasize the strong correlation between thermal gradients and stress behavior, highlighting the importance of monitoring and controlling temperature distributions to minimize stresses within the slabs during their heating process. As shown by the graph in Fig. 12, at slab 3 the normalized difference was around 80% difference in the top vs. core temp, while at the highest magnitude at slab 12, the percentage was half, around 37%.

The stress distribution along the core of the slab has been plotted at four different slab positions. This revealed that there are distinct stress peaks at specific locations where the skids are located on which the slabs rest. These peaks represent areas where the temperature gradient

Figure 13

Stresses along longitudinal axis at specific slab positions in the furnace.

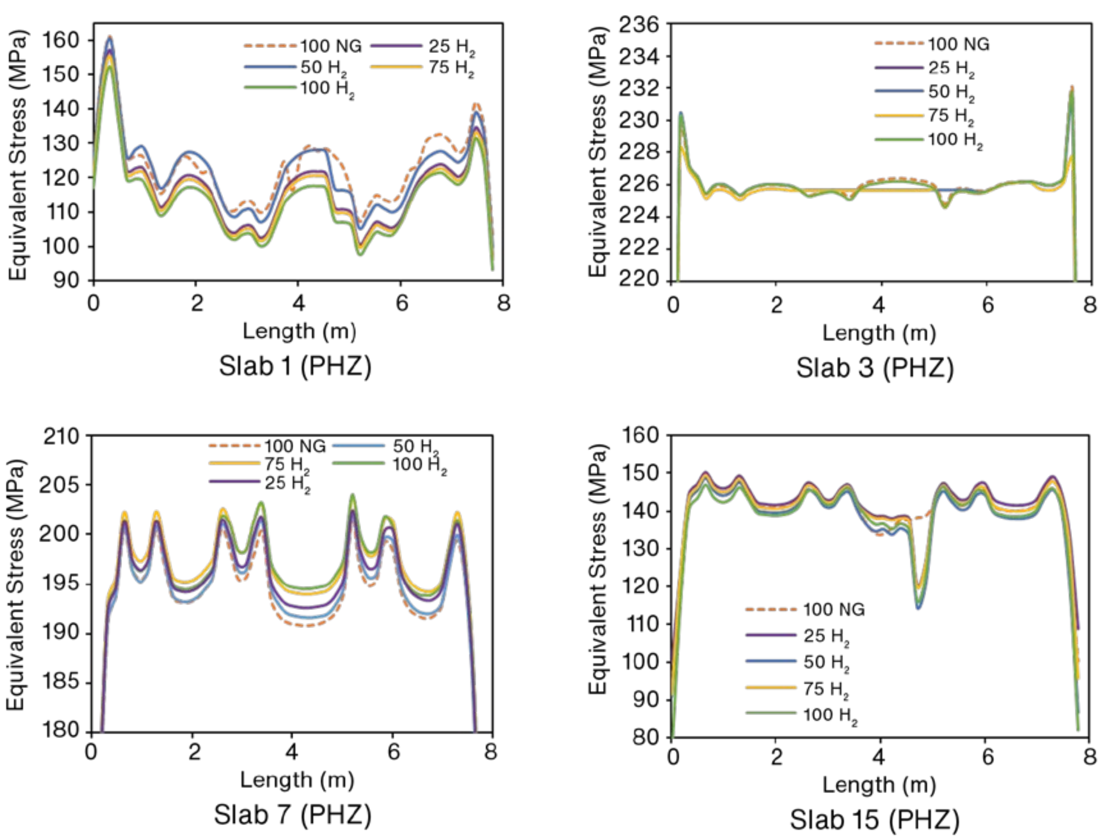

throughout the slab was the highest due to skid cooling effects, thus also causing higher thermal stresses in those areas.

However, when the slabs transition into HZ1, the stress distribution remains relatively uniform. Minimal differences in stress values are observed, indicating that the entry into HZ1 does not significantly affect the overall stress profile along the core.

Conclusion

Based on the findings, hydrogen's use as a fuel in reheat furnaces presents both opportunities and challenges. While hydrogen minimally impacts slab stress compared to methane, its influence on thermal gradients is substantial, particularly in the early stages of the furnace, where the highest stresses are observed. The significant thermal gradients observed, such as those around slab 3, align with peak stress values, emphasizing the correlation between thermal and mechanical behaviors. However, as the slabs progress through the furnace, temperature distribution homogenizes, reducing stress levels and ensuring slabs remain within the elastic deformation range.

Hydrogen's higher combustion temperatures and radiative heat transfer efficiency lead to increased thermal inputs to the slabs, resulting in elevated temperature gradients. This requires careful management of hydrogen input rates to achieve consistent slab exit temperatures comparable to natural gas. These results highlight the need for optimized furnace designs and operational strategies to balance the benefits of decarbonization with the mechanical integrity of steel slabs. By providing insights into the thermal and stress implications of hydrogen integration, this study supports the steel industry's transition to cleaner, sustainable fuel sources without compromising product quality or process efficiency.

Acknowledgment

This material is based on work supported by the U.S. Department of Energy's Office of Energy Efficiency Renewable Energy (EERE) under Award Number DE-EE0010843.

Legal Disclaimer

This article is available online at AIST.org for 30 days following publication.

References

1. P. Marocco, M. Gandiglio, D. Audisio and M. Santarelli, "Assessment of the Role of Hydrogen to Produce High-Temperature Heat in the Steel Industry," *Journal of Cleaner Production,* Vol. 388, Art. No. 135969, 2023.
2. A. Kolakotla, N.J. Walla, A.K. Silaen, L. Fabina, K. Johnson and C.Q. Zhou, "Computational Modeling of H_2/CH_4 Combustion in a Slab Reheating Furnace," *Proceedings of the 3rd International Symposium on the Recent Developments in Plate Steels,* 2024, pp. 247–257, https://doi.org/10.33313/300/025.
3. A. Karambelkar, C. Uzor, N. Walla, A. Silaen, L. Fabina, K. Johnson and C. Zhou, "Decarbonization and Increased Productivity in the Reheating Furnace Using Hydrogen Fuel," *AISTech 2023 Conference Proceedings,* 2023, https://doi.org/10.33313/387/229.
4. C. Uzor, "Characteristics of Hydrogen Fuel Combustion in a Reheating Furnace (Version 1)," Purdue University Graduate School, 2022, https://doi.org/10.25394/PGS.21711737.v1.
5. F.J.M. Zambrano, B. Worl, X. Li, A.K. Silaen, N. Walla, K. Johnson, L. Fabina and C. Zhou, "Numerical Analysis of Thermal Stress Development of Steel Slabs in a Pusher-Type Reheat Furnace," *Proceedings of the ASME 2020 Heat Transfer Summer Conference co-located with the ASME 2020 Fluids Engineering Division Summer Meeting and the ASME 2020 18th International Conference on Nanochannels, Microchannels, and Minichannels,* Vol. 1, Article V001T02A004, 2020, https://doi.org/10.1115/HT2020-9093.
6. ANSYS® Fluent Theory Guide, Release 23R1, ANSYS Inc. ✦

AISTech This paper was presented at AISTech 2025 — The Iron & Steel Technology Conference and Exposition, Nashville, Tenn., USA, and published in the AISTech 2025 Conference Proceedings.